World Academy of Science, Engineering and Technology
International Journal of Aerospace and Mechanical Engineering
Vol:8, No:12, 2014

In-situ Quasistatic Compression and Microstructural Characterization of Aluminum Foams of Different Cell Topology

M. A. Islam, P. J. Hazell, J. P. Escobedo, M. Saadatfar

***Abstract*—**Metallic foams have good potential for lightweight structures for impact and blast mitigation. Therefore it is important to find out the optimized foam structure (i.e. cell size, shape, relative density, and distribution) to maximise energy absorption. In this paper, quasistatic compression and microstructural characterization of closed-cell aluminium foams of different pore size and cell distributions have been carried out. We present results for two different aluminium metal foams of density 0.49-0.51 g/cc and 0.31-0.34 g/cc respectively that have been tested in quasi-static compression. The influence of cell geometry and cell topology on quasistatic compression behaviour has been investigated using optical microscope and computed tomography (micro-CT) analysis. It is shown that the deformation is not uniform in the structure and collapse begins at the weakest point.

***Keywords*—**Metal foams, micro-CT, cell topology, quasistatic compression.

I. Introduction

THE extraordinary combination of mechanical properties of metal foam has attracted many potential applications involving shock and impact loading. In recent years, the focus on metal foams has been intensified due to their higher strength and stability in thermal, mechanical environment in comparison to other porous structures such as polymer and ceramics foam [1].Various modes of manufacturing of metal foams has been developed for different metals such as aluminum, magnetism, titanium and copper. Among them aluminum foams gain more attention and interest because of their high-energy-absorption–to-weight-ratio. The mechanical properties of aluminum foam structures have been investigated extensively in the past decade both dynamically and quasi-statically [2]-[9]. Fundamental macroscopic analysis of foam structure has been done by Ashby et al. [10]. They showed that the material density variation determined the mechanical properties of the cellular structure. However, subsequent studies [11]-[14] showed that not only material density but also microscopic features influence the performance of closed-cell aluminium foams. It has been found that some of the crucial cell parameters such as morphology and distribution [15]; topology (cell-neighbor relationship) and cell size [16]; cell orientation and cell-wall thickness [17] (curvature and corrugation); cell-wall roughness [18]; micro-pores in the cell-wall and cell-wall material properties (inclusions and dislocation) [19] determine the overall performance and integrity of the foam.

Furthermore, the structure of closed-cell aluminum foam is complex. The gas entrapped inside the cell enhances the strength as the gas is compressed during compressive loading. The deformation of closed-cell aluminum foam gives the elastic-plastic characteristics and large deformation during pore collapse results in substantial energy absorption. Fig. 1 shows the ideal stress-strain curve of closed-cell aluminum foam which represents three steps of compression: a. Elastic compression, b. plastic deformation and c. material densification (collapse of cell void space).

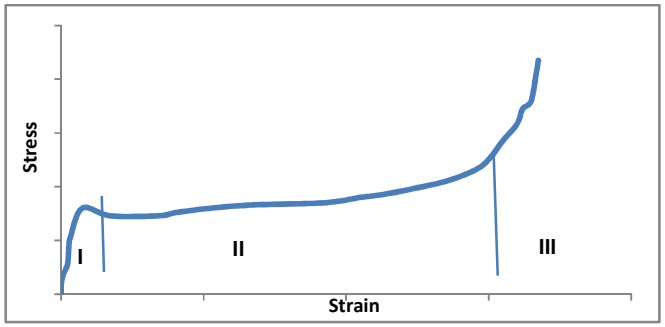

Fig. 1 Ideal stress- strain diagram for closed-cell aluminum foam: I. Linear elastic compression, II. Plastic collapse,and III. Densification

Although this macroscopic view of metal foam deformation is well established, the microscopic deformation mechanism at different strain rates and its effect on overall foam performance had not yet established adequately. Mu et al. [20] suggests the deformation process of closed-cell aluminum foam initiated with crumbling the cell wall in compression direction. Cao et al. [16] found that the cell size has substantial influence on strain rate sensitivity; they also found that foams of average cell size have larger modulus and compressive strength under both quasistatic and dynamic state. Ruan et al. [21] and Sugamura et al [22] showed that two factors influence the mechanical performance of closed-cell foam: a. Cell wall material b. Presence of gas inside the cell (which increases the modulus and plateau stress).

All of the above literature provides the list of parameters that influence the structural performance of metal foams.

M. A. Islam, P. J. Hazell, are J. P. Escobedo-Diaz with with the School of Engineering and Information Technology, UNSW Canberra, Australia (e-mail: md.islam4@student.adfa.edu.au, p.hazell@adfa.edu.au, J.Escobedo-Diaz@adfa.edu.au).

M. Saadatfar is with the Department of Applied Mathematics, Australian National University, Canberra, Australia (e-mail: mohammad.saadatfar@anu.edu.au).

However, to achieve optimized foam structure all the foam parameters need to be improved, this requires proper macro and micro characterization of metal foams. This paper presents the characterization data of closed-cell aluminium foam from the microstructural point of view. Also, compressive failure and micro-structural change during the compression have been revisited.

II. Initial Material Characterisation

Two different stabilized CYMAT aluminium foams (produced via melt route) with nominal densities of 0.51 g/cc and 0.36 g/cc have been tested. The provided foam has solid layer of aluminium skin in the upper and lower surface of the foam sheet. For obtaining the homogeneity in all the region of the test sample, the upper and lower surface skins were removed. After removing the skins, sample density remained approximately 0.48 g/cc -50 g/cc and 0.31 g/cc-0.33 g/cc respectively. For convenience, we designate the foam of density range 0.48 g/cc to 50 g/cc as HD (higher density) and foam of density range 0.31 g/cc to 0.33 g/cc as LD (low density). The measured physical properties of the given foams are shown in Table I. The nominal dimensions of the samples were 40 mm×40 mm×23 mm for both foams which were cut using electro discharge machining (EDM) to avoid distortion in the sample boundary.

TABLE I
Measured Physical Properties of Supplied Closed- Cell Foam

Name	HD	LD
Density (g/cc)	0.48-0.51	0.31-0.35
Relative density (%)	17.00-18.80	11.40 – 12.90
Porosity (%)	81.20 – 83.00	87.10-88.60
Mean Cell-size (mm)	1.75	3.95
Std. dev. of cell-size (mm)	1.13	1.98
Wall thickness (mm)	0.10-0.23	0.10-0.21

Fig. 2 shows the test sample of LD foam of density 0.31 g/cc. The entire compressive test was performed along Z-direction. The local density of foam was not same along Z-direction, although X and Y direction found fairly homogeneous distribution. Fig. 3 shows the general foam structure of the supplied CYMAT foam.

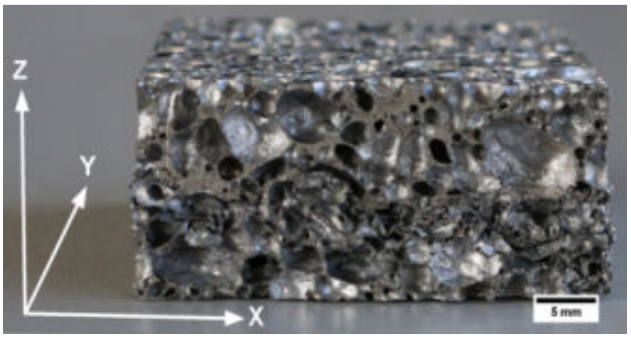

Fig. 2 Test sample of LD (density 0.29g/cc), uniaxial compressive test was performed alone Z-direction

Fig. 3 reveals the cell size distribution over the foam structure. It is shown that the cell size variation along Z-direction is noticeable than X and Y direction. It also was found that the range of cell-size (smallest to highest diameter) is higher for lower density foam (LD) than the higher density foam (HD). However, in higher density foam, density distribution is more inhomogeneous than the low density foam as shown in the Fig. 3.

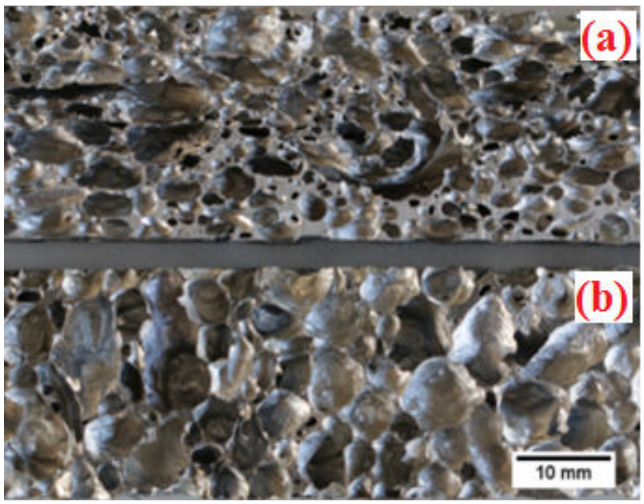

Fig. 3 Supplied aluminium foam structure (surface perpendicular to axis of compression: (a) HD density 0.49 g/cc and (b) LD density 0.31 g/cc

The cellular network has been measured by using high resolution X-ray computed tomography. The foam samples for the micro-CT were the same samples used in compressive test. After scanning process was done by CT- X-ray, the images were transmitted to the detector. Then a series of 2D X-ray projections were collected with the small fraction of degree of rotational orientation of the sample. The image reconstruction was made by means of qmango and ncviwer software which is located at the Department of Applied Mathematics, the Australian National University. Image analysis processes of scanned tomographic data were carried out in the following steps: firstly the x-ray image was filtered and then masked; the image was then watershed and partitioned. Finally the skeletal images of foam structure were taken to observe the cell network.

The tomographic data (Fig. 4) shows the morphological and topological features of the tested closed-cell aluminium foam. It has been found that the cell shape does not follow the specific geometrical shape however it can approximately be considered as elliptical. Zhang et al. [23] calculated the cell shape as spherical for the convenience of calculation. However, in our work we measured the average cell area using ImageJ software then the characteristics cell size were measure by image analysis. Once the cell-size was measured, the cell size-distributions for our experimental foam were plotted which are shown in the Fig. 5. It has been observed that the average cell-size for HD was around 1.75 mm to 2 mm and for the LD approximately 3.75 mm to 4.00 mm. The

range of cell–wall for the HD was 0.1 mm to 5.5 mm whereas for the LD foam, it was 0.25 mm to 9.5 mm.

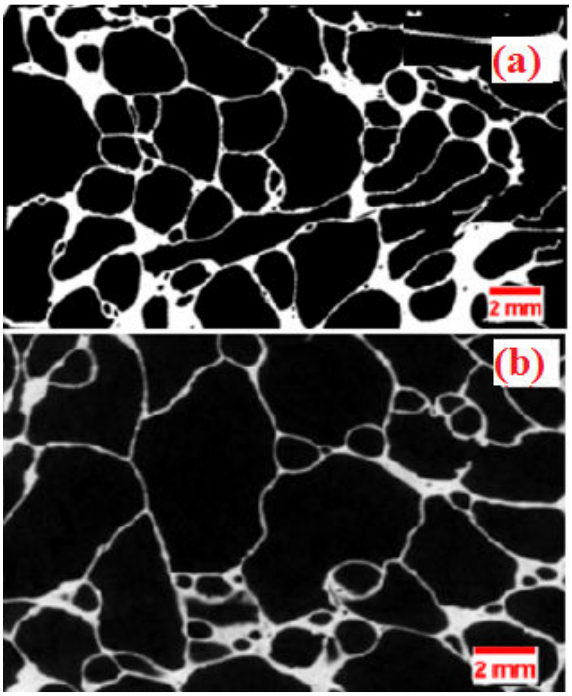

Fig. 4 The micro- CT data of closed-cell aluminium foam showing the distribution and cell structure: (a) HD (density 0.49 g/cc) and (b) LD (density 0.29 g/cc)

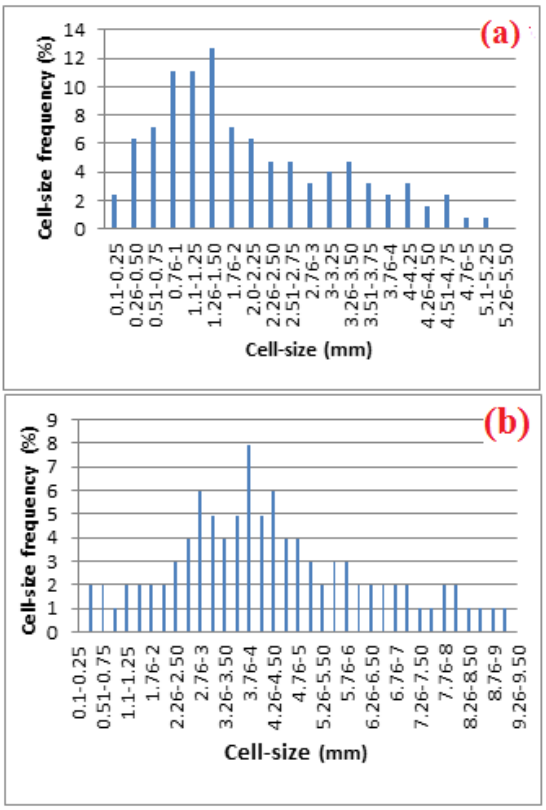

Fig. 5 Cell-size distribution of the foam structure: (a) HD (density 0.49 g/cc) and (b) LD (density 0.29 g/cc)

Fig. 6 shows the cell wall and cell wall composition of our tested sample of density 0.49 g/cc. Some wiggle and kinks have been found in the wall as shown in the Fig. 6. The dark spot in the cell wall indicated the irregularities and corrugation which is predominant near the edge of the wall. Also, the micrograph indicated that the cell wall is not smooth. Furthermore the cell-wall thickness varied within the network. This fact is probably due to the gas pressure during the foam solidification process. Experimental failure of closed-cell aluminium during compression revealed that the cell collapse starts at the position where the wall material thickness is lowest.

Another imperfection noticed in the closed-cell foam was micro-pore near the cell-wall edge. The cell wall has some micro-pores which were observed from the microscopic image of the cell-wall (Fig. 6).

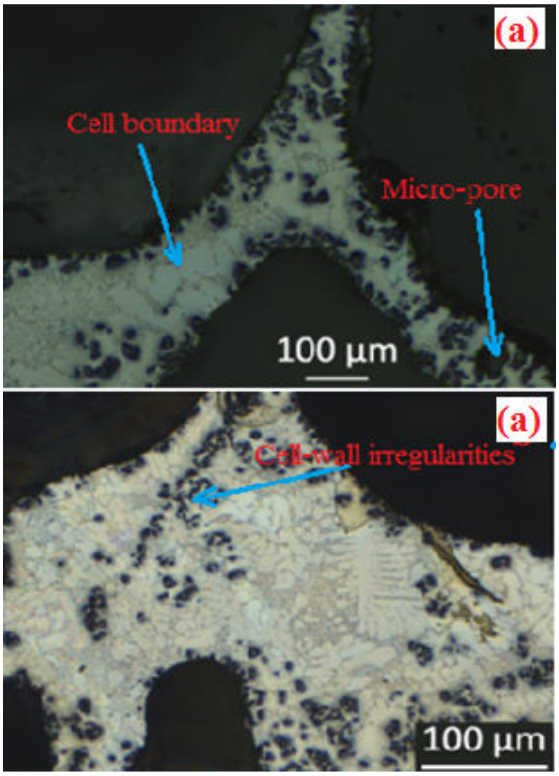

Fig. 6 Microstructural image of cellular network and cell-wall of HD (density 0.49 g/cc): (a) cell-wall joint and (b) cell-wall surface

III. Quasi-Static Testing

Firstly, the weight and dimension of individual EDM cut sample was measured before compression test. The final sample size and density of individual samples are given in Table II which shows that sample density is not the same as the density of its parent foam sheet. This was due to the variation of cell-size over the structure. After measuring the dimension and density of individual samples, the sample is placed between two fixed parallel platens of a Shimadzu universal testing machine. The integrated high-speed camera was used to observe the cell collapse and overall deformation during the compression. Uniaxial compression load was

applied with the constant cross-head velocity of 1.4 mm/sec, this translated to a constant strain-rate of 10^{-3} s^{-1}.

Compressive tests were performed to strain-rate of 15%, 25% and 45%, 60 %) to observe the elastic, plastic and densification stages. The sample size was at least 10 times greater than the cell-size for the HD foam and 6 times for LD foam to avoid the size effect. After the compression test, the deformed samples were observed under a microscope. This is discussed in the results and discussion section.

TABLE II
MEASURED DIMENSION AND DENSITY OF TESTED SAMPLE

Sample	Measured Density (g/cc)	Measured Dimension (mm)
HD	0.480	39.7x40.10x23.10
	0.490	39.72x41.05x23.18
	0.485	39.68x39.78x23.13
	0.505	39.7x40.14x23.15
LD	0.313	40.10x40.20x23.19
	0.314	40.05x40.15x23.21
	0.320	40.15x40.2x23.02
	0.344	40.20x40.21x23.23

IV. RESULTS AND DISCUSSION

The stress-strain curve of the foam of different density has been demonstrated in Fig. 7 (a). It was observed that the stress-strain curves followed almost the similar pattern of ideal-stress strain curve of a metal foam i.e. it exhibited three regions: an initial linear elastic region; an extended plateau state and final densification due to cell collapse. However the foam with the lower density had an ideal (lower) plateau stress. The plateau stress for the higher density foam constantly rose although the stress remained constant for the lower density foam. Nonetheless, it was found that the deformation characteristics followed the same pattern to those of other closed-cell aluminium foams available the literature.

It has been observed that the linear elastic deformation region reached peak at around 0.5% to 1.5% of the strain. In this region aluminium foam acted as an elastic material and it has been observed that the deformation mechanism in this stage was limited to flexural bending of the cell wall. However, as the load rises, the foam reached yield and sudden decrease of stress is followed before a stable plateau of stress due to plastic collapse. It was observed that plastic deformation took place successively (asynchronously) in the closed-cell aluminium structure. The plastic collapse stage is the longest stage. This phase of compression was maintained for almost the entire foam deformation (nearly from 2% to 60% strain). This large deformation phase absorbed the significant amount of plastic energy.

During the compression test, live camera showed that plastic deformation process started in the region of the foam where the material's density is low (big cell size and large void space) and high heterogeneous cell distribution. It was seen that the commencement of cell collapse started in the middle part of the foam structure almost in every sample. It was also found that the deformation in this stage is a continuous process of cell-wall buckling, yielding and fracturing. As soon as the cell-wall fractured the entrapped gas is released from the cell and the compaction of material took place by occupying the cell void by the compacted cell wall materials. With the increase in strain, the neighboring cells of a compacted layer followed the same route. Thus the process described above repeated until all of the cells of the sample collapsed.

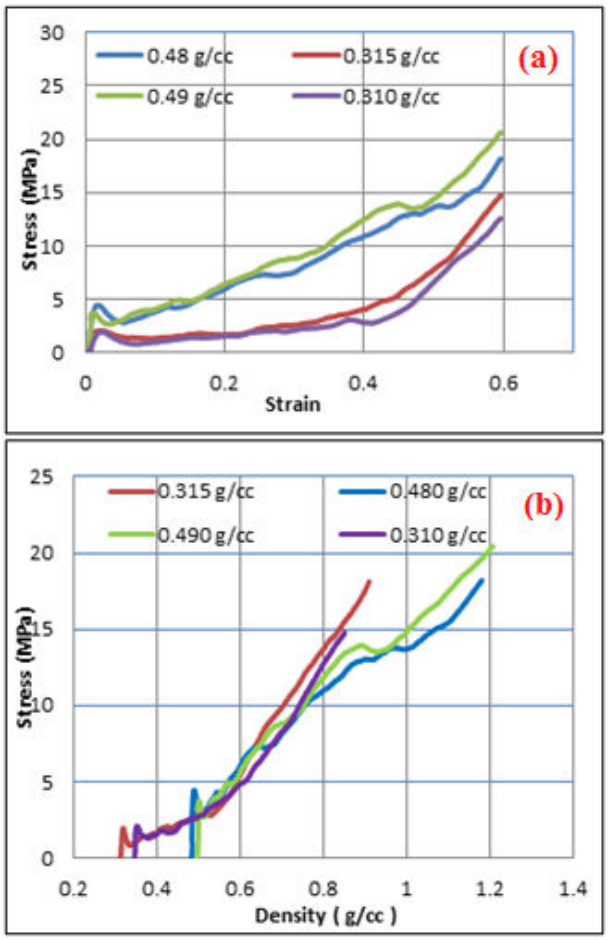

Fig. 7 Quasi-static test results (a) Stress-strain curve (b) stress-density curve

After the end of plateau phase, the compacted collapse region cannot deform much further as all the cell void is occupied by the cell wall. In this region, the stress rises significantly with little increase in strain. Fig. 7 (a) shows the four stress–strain curves for HD and LD foam, where foams with density 0.315 g/cc and 0.310 g/cc follow similar loading paths that sit lower than the HD foams. With the increase of foam density, the foam started to deviate from the plateau stage towards its parent metal's characteristics. This observation also corroborated by other higher density foam experiments performed by [17]. It has been shown that the LD foam has almost an ideal plastic region (plateau); however the HD foam absorbed more energy as a relatively high stress is required for its deformation (indicated by the high position of the loading path in the stress-strain graph).

The stress-density curves for the HD and LD foam as

shown by Fig. 7 (b) reveal that during the plastic compression regardless of primary foam density the stress become similar for the same density. This indicates that the closed-cell aluminium foam's strength highly depends of density of the foam.

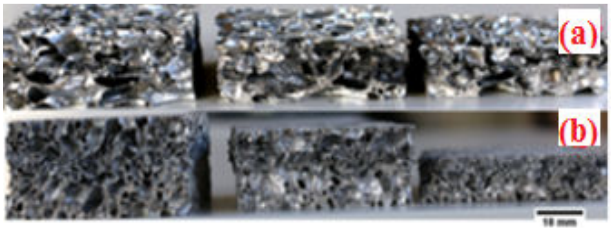

Fig. 8 15%, 25% and 45% deformed sample (start from left to right): (a) HD (bottom) and (b) LD (top)

Fig. 8 shows the 15%, 25% and 45 % deformed sample. It is shown that all the sample start to deform where the cell walls are weak and density is low (large pore) which indicate the necessity of homogeneity of cell distribution and cell-wall material thickness over the foam structure.

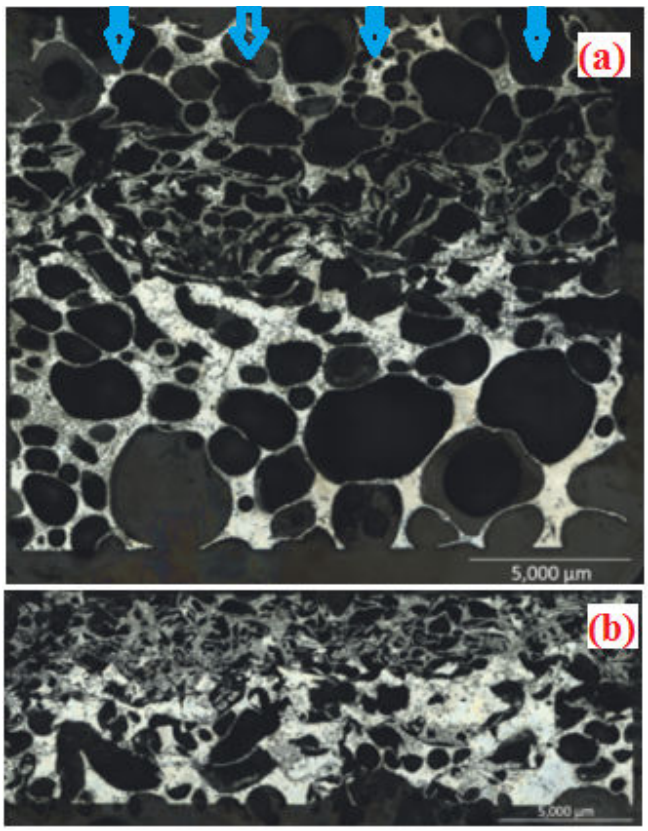

Fig. 9 Microscopic image of cell deformation during compression (a) 25% compressed sample (b) 60% compressed sample

Fig. 9 shows the pore collapse of foam surface (HD) along the direction of compression. It was observed that the cell deformation initiated from the weakest region of the foam propagating from top to bottom in the downward direction (compressive loading direction). Fig. 9 (a) shows 25% compressed and Fig. 9 (b) shows the 60% compressed sample. The cells have been compressed and become flattened along the loading direction. However it was found that the surface perpendicular to the loading direction expanded and fractured. It was also observed that at the densification stage, cell walls disintegrate and expanded towards the periphery.

V. Conclusion

The following conclusions can be drawn from our quasi-static compression experiments on closed-cell aluminium foams

- The closed-cell aluminium foam structure is heterogeneous and the cell distribution is irregular which means the cell orientation varies throughout the foam height.
- The deformation is not uniform in the entire region of the sample. That is, deformation initiated at the weakest point in the sample and propagated from this region until densification. Also, the cell-wall material under high stress is weakened and consequently the cell wall becomes flattened which results in significant expansion in the lateral direction.
- The loading capacity of the foam depends on the density of the foam. The regular structure of the foam provides better performance. For the low density foam, the stress-strain diagram is smoother but the energy absorption capacity is not large (Fig. 7 (a))
- Performance of the closed-cell foam can be enhanced by minimizing the structural defect and optimizing the structural parameters such as regular cell distribution and smooth cell-wall materials.

Acknowledgments

The authors gratefully acknowledge David Sharp and Mathew Barrett of Material testing Lab. of UNSW Canberra for their countless assistance in material testing and technical support by Jill Middleton, Department of Applied Mathematics, The Australian National University, Canberra, Australia.

References

[1] H.P. Degischer, B.E. Kriszt, "Handbook of Cellular Metals: Production, Processing Applications," in *Willy-VCH*, 2002.
[2] E. Raj, V. Parameswaran and B.S.S. Daniel, "Comparison of quasi-static and dynamic compression behavior of closed-cell aluminum foam," *Materials Science and Engineering*, vol. A.526 (1-2), 2009, pp. 11-155.
[3] E. Raj and B.S.S. Daniel, "Customization of closed-cell aluminum foam properties using design of experiments," *Materials Science and Engineering*, vol. A.528 (4-5), 2011, pp. 11-155.
[4] P.J. Tan, S.R. Reid, J.J. Zou and S. Li, "Dynamic compressive strength properties of aluminium foams. Part II - 'shock' theory and comparison with experimental data and numerical models," *Journal of the Mechanics and Physics of Solids,* vol. 53(10), 2005, pp. 2206-2230.
[5] L.J. Gibson and M.F. Ashby, "Cellular solids: structure and properties," *Cambridge university press.* 1999.
[6] H Toda , T Kobayashi,N. Niinomi,T Ohgaki, M. Kobayshi, N. Kuroda, and Y. Aruga, "Quantitative assessment of microstructure and its effects on compression behaviour of aluminum foams via high-resolution synchrotron X-ray tomography," *Metallurgical and Materials Transactions,* vol. 37(4), 2006, pp.1211-1219.

[7] P. Kenesei, C. Kádár, Z. Rajkovits, and J. Lendvai, "The influence of cell-size distribution on the plastic deformation in metal foams,". *Scripta Materialia*, vol. 50(2), 2004, pp. 295-300.
[8] C. Kádár, E. Maire, A. Borbély, G. Peix, J. Lendvai, and Z. Rajkovits "X-ray tomography and finite element simulation of the indentation behavior of metal foams,". *Materials Science and Engineering,* vol. A, 387-389 (1-2), 2004, pp.321-325.
[9] R.P. Merrett, G.S. Langdon, and M.D. Theobald, "The blast and impact loading of aluminium foam," *Materials and Design,* vol. 44, 2003, pp. 311-319.
[10] M.F. Ashby, A.G. Evans, N.A. Fleck., L.J. Gibson, "Metal Foams: a design guide," *Huchinson, J.W. & Wadley*, H.N.G. Butterworth-Heinemann. Publications, 2000.
[11] M.F. Ashby, R.F. M. Medalist, "The mechanical properties of cellular solids," *Metallurgical Transactions*, vol. A, 14(9), 1983, pp.1755-1769
[12] E. W .Andrews, C. Gioux, P.R. Onck and L.J. Gibson, "Size effect in ductile cellular solids, Part II: experimental results," *Int. J. Mech. Sci.* vol. 43, 2001, pp.701–713.
[13] C. Chen, N.A. Fleck Size effects in the constrained deformation of metallic foams*, Journal of the Mechanics and Physics of Solids,* vol. 50, 2002, pp.955 – 97.
[14] A.F. Bastawros, H.B. Smith and A.G. Evans, "Experimental analysis of deformation mechanics of closed-cell aluminium alloy foam," *J. of Mechanics and Physics of Solids,* vol. 48, 2000, pp.301-322.
[15] P. Kenesi, C. Kadar, Z. Rajkovits and J. Lendvai, "The influence of cell-size distribution on the plastic deformation in metal foams" *Scripta Materialia,* vol. 50, 2004, pp.295-300.
[16] X. Cao, Z. Wang, H. Ma and L. Zhao, "Effects of cell size on compressive properties of aluminium foam," *Trans. Nonferrous Met. Of China,* vol. 16, 2006, pp.351-356.
[17] M.R. Said and C. Tan, "The response of Aluminium Foams under Quasi-static loading," *Chiang Mai J. Csi*., Vol. 35(2), ,2008, 241-249
[18] A.E. Markaki and T.W. Clyne, "The effects of cell wall microstructure on the deformation and fracture of aluminium-based foams," *Acta Materilia,* vol. 49, 2001, pp.1677-1686.
[19] I. Jeon, K. Katou, T. Sonoda, T. Asahina, and K.J. Kang, "Cell wall mechanical properties of closed-cell Al foam," *Mechanics of Materials,* vol. 41(1), 2009, pp.60-73.
[20] Y. Mu, G.Yao,L. Liang , H. Lou and G. Zu , " Deformation of close-cell aluminium foam in compression" *Scriptal Materilia,* vol.63, 2010, pp. 629-632.
[21] D. Ruan, G. Lu, F.L. Chen, E. Siores, " Compressive behavior of aluminium foams at low and medium strain rates" , *J. Composite Structures,* vol. 57, 2002, pp. 331-336.
[22] Y. Sugamura , J. Meyer, M.Y. He, H. Bart-smith, J. Grenstedt and A.G. Evans, "On the mechanical performance of closed cell Al alloy foam." *Acta Materilia*, vol.45 (12), 1007, pp.5245-5259.
[23] Q. Zhang, P.D. Lee, R. Singh, G. Wu and T.C. Lindley, "Micro-CT characterization of structural features and deformation behavior of fly ash/aluminium syntactic foam," *Acta Materialia,* vol. 57, 2009, pp.3001-3011.